Environ. Sci. Technol. **2005**, *39,* 8288−8294

Zinc Sorption by a Bacterial Biofilm

BRANDY TONER,*,† ALAIN MANCEAU,‡ MATTHEW A. MARCUS,§ DYLAN B. MILLET,|| AND GARRISON SPOSITO†

Department of Environmental Science, Policy, and Management, Division of Ecosystem Sciences, University of California, Berkeley, California 94720-3114, Environmental Geochemistry Group, LGIT − Maison des Geosciences, Université J. Fourier and Centre National de la Recherche Scientifique (CNRS), B.P. 53, 38041 Grenoble Cedex 9, France, Advanced Light Source, Lawrence Berkeley National Laboratory, Berkeley, California 94720, and Department of Earth and Planetary Sciences, Harvard University, Cambridge, Massachusetts 02138

Microbial biofilms are present in soils, sediments, and natural waters. They contain bioorganic metal-complexing functional groups and are thought to play an important role in metal cycling in natural and contaminated environments. In this study, the metal-complexing functional groups present within a suspension of bacterial cell aggregates embedded in extracellular polymeric substances (EPS) were identified in Zn adsorption experiments conducted at pH 6.9 with the freshwater and soil bacterium *Pseudomonas putida*. The adsorption data were fit with the van Bemmelen−Freundlich model. The molecular speciation of Zn within the biofilm was examined with Zn K-edge extended X-ray absorption fine structure (EXAFS) spectroscopy. The Zn EXAFS data were analyzed by shell-by-shell fitting and linear least-squares fitting with reference spectra. Zinc sorption to the biofilm was attributed to predominantly Zn−phosphoryl (85 ± 10 mol %) complexes, with a smaller contribution to sorption from carboxyl-type complexes (23 ± 10 mol %). The results of this study spectroscopically confirm the importance of phosphoryl functional groups in Zn sorption by a bacterial biofilm at neutral pH.

Introduction

Microorganisms in aquatic environments adhere to one another and to surfaces and interfaces (*1*, *2*), embedding themselves in extracellular polymeric substances (EPS) (*3*). The ubiquity of this biofilm growth habit has been verified by extensive direct observation in natural aquatic environments (*1*, *2*). Due to greater recognition of their importance in environmental processes, the study of biofilms has increased dramatically in the past decade (*3*). However, biofilms possess physical structure, biological complexity, and chemical heterogeneity, all of which lead to significant analytical challenges for researchers (*3*).

* Corresponding author. Current address: Department of Marine Chemistry and Geochemistry, Woods Hole Oceanographic Institution, Woods Hole, MA 02543. E-mail: btoner@whoi.edu; fax: (508)457-2013.

† University of California.

‡ Université J. Fourier and CNRS.

§ Lawrence Berkeley National Laboratory.

|| Harvard University.

There is a rich body of literature describing metal sorption from aqueous solution by bacterial cells through wet chemistry experimentation. Often these metal sorption studies are combined with acid−base titrations and modeling to characterize the proton- and metal-exchanging sites on the bacterial cell surface(s). Studies such as these indicate that bacteria likely play an important role in metal speciation in environmental (*4*, *5*) and industrial settings (*6*). However, modeling of metal sorption data alone does not provide a mechanistic understanding of metal complexation by bacterial surface functional groups—spectroscopic examination is required (*7*). Few spectroscopic studies of metal sorption by bacteria have been conducted. In addition, despite the demonstrated importance of biofilms in metal sequestration, (e.g., refs *8* and *9*), little research on metal sorption by bacterial biofilms has been conducted by wet chemistry or spectroscopy.

X-ray absorption spectroscopy (XAS) is a useful tool for the study of metal speciation as it provides information about the local molecular structure of the metal of interest, in principle providing the identity of aqueous, sorbed, and precipitated species. Application of XAS to biofilm studies is particularly useful because metal speciation can be determined in unprocessed samples within complex substrates having variable or poorly defined organic and inorganic components.

In previous work with the *Pseudomonas putida* strain MnB1 culture, we studied Zn sorption and speciation in the presence of biogenic Mn oxides (*10*). We found that Zn preferentially partitions to the biogenic Mn oxide, saturating the oxide surface sites before Zn sorption to bioorganic material is observed. However, after Mn oxide saturation the bioorganic functional groups present in the biofilm contribute significantly to Zn sorption, accounting for up to 38 mol % of Zn sorption at pH 6.9; the identity of the bioorganic Zn-complexing functional groups was not determined in that study.

In the present study we conducted Zn adsorption isotherm experiments at pH 6.9 and used Zn K-edge extended X-ray absorption fine structure (EXAFS) spectroscopy to examine the molecular speciation of Zn sorbed to bacterial cell aggregates of *P. putida* embedded in EPS. This research provides information on the molecular speciation of Zn within a biofilm setting and spectroscopically confirms the importance of phosphoryl-type functional groups in Zn complexation by bacterial biofilms at neutral pH.

Materials and Methods

Zn Adsorption Isotherm. *P. putida* strain MnB1 was grown in liquid medium for 7 days at 27 ° C under rotary shaking at 150 rpm (see ref *11* for details). The cells aggregate during the exponential phase of growth and produce EPS during the exponential and stationary phases of growth (*12*). Sample suspensions were prepared for the adsorption isotherm experiments with two centrifuge-and-rinse cycles (in sterile 250 mL polypropylene copolymer bottles for 30 min at 10 200 RCF) with sterile pH 7, 0.01 M NaCl solution. Microscopic examination of cell aggregates (with biogenic Mn oxides present in the biofilm), rinsed with 0.01 M NaCl and exposed to Zn, reveals an EPS coating around the cell aggregates very similar to that observed for unrinsed cell aggregates (data not shown); this suggests that the electrolyte rinses do not remove the EPS coating from the cell aggregates. The sample suspensions were adjusted to pH 7.0 with additions of sterile 0.1 M NaOH and 0.1 M HCl and equilibrated overnight. The sample suspensions were diluted gravimetrically to a density

10.1021/es050528+ CCC: $30.25
Published on Web 09/24/2005

of 0.03 g of dry biofilm L^{-1} and weighed into sterile 250 mL Teflon bottles (Nalgene) containing Teflon-coated stir bars. Experiments were performed with undried biofilm suspensions, while the amount of biosorbent per liter of suspension was determined with a subsample of suspension by centrifuging, decanting the electrolyte solution, and drying at 70 °C for more than 24 h. Additions of $ZnCl_2$ were made gravimetrically from a stock solution (pH 4.0, 0.01 M Zn). Controls without solids at low and high Zn concentrations were prepared in Teflon bottles (no measurable Zn was sorbed by these containers). The samples (nine Zn concentrations per experiment, with each experiment repeated three times) were placed on magnetic stirring platforms at room temperature (20 ± 2 °C). The pH was monitored at least four times daily and maintained at 6.90 ± 0.15 by additions of sterile 0.1 M NaOH or 0.1 M HCl. The solution-phase Zn concentration was measured 48 h after the pH stabilized by removing an aliquot of sample suspension while stirring vigorously. The aliquot was filtered, acidified, and analyzed by inductively coupled plasma−atomic emission spectrometry (ICP-AES, IRIS Thermo Jarrell Ash). All solutions were prepared in MQ water (MilliPore Milli-Q, 18.2 MΩ·cm).

The Zn removed from solution by the biofilm (q, moles of Zn per kilogram of biosorbent) was quantified with the equation $q = ([Zn]_0 - [Zn]_t)[\text{biosorbent}]^{-1}$, where $[Zn]_0$ and $[Zn]_t$ are the solution-phase Zn concentrations at time zero and at the sampling time (moles of Zn per liter) and [biosorbent] is the total mass (kilograms) of biofilm in the sample suspension per liter. After a careful examination of alternative models (see Supporting Information), the Zn sorption data were fit to the van Bemmelen−Freundlich equation (*13*) $q = Ac^{\beta}$, where A is an adjustable scale factor with appropriate units, c is the equilibrium Zn concentration in moles of Zn per kilogram of suspension, and β is a dimensionless adjustable heterogeneity parameter ($0 < \beta \leq 1$). Nonlinear least-squares fits to the Zn sorption data, q versus c, were performed to obtain values for A and b with standard errors. The fitting and estimation of 95% confidence intervals was performed with S-Plus v 6.2 (Insightful Corp.) software.

Zn K-Edge EXAFS Spectroscopy. Zinc K-edge EXAFS spectra of experimental samples were collected at beamline 10.3.2 at the Advanced Light Source (ALS), Lawrence Berkeley National Laboratory (LBNL) (*14*). The spectra were collected under air-dry conditions in fluorescence mode with a 7-element germanium detector. Samples from the adsorption experiments were prepared by collecting the solid material as a paste onto a membrane filter and wicking away the entrained solution. Potential effects of air-drying the samples on Zn speciation were not examined; Zn EXAFS spectra have been collected successfully from air-dried samples in a similar study (*15*). The Zn EXAFS experimental and reference spectra [$\chi(k)$] were processed and analyzed with SixPack software (*16*). The spectra were k^3-weighted and Fourier-transformed {FT[$\chi(k)k^3$]} in the k range of 3−13 $Å^{-1}$. The real and imaginary parts of FT[$\chi(k)k^3$] were interpreted with shell-by-shell fitting by use of phase and amplitude functions calculated with FEFF6 (17). The quality of each structural fit was evaluated quantitatively by the reduced chi square (χ_ν^2) and R-factor parameters (*18*). All fitted parameters [interatomic distance R (angstroms), coordination number N, and mean-square displacement of bond length σ^2 (angstroms^2)] are presented with the estimated errors from IFEFFIT calculations (*19*). In these fits to the experimental spectra, the amplitude reduction factor (S_0^2) was set to 0.9.

Linear least-squares fitting of k^3-weighted experimental EXAFS spectra with reference spectra also was conducted. The numerical results of these linear fits estimate the fractional contribution of each reference spectrum to the experimental spectrum with a precision of approximately ±10% of total Zn (*20*), the goodness of fit being assessed by the χ_ν^2 parameter. The reference spectra used in this study have been described in previous publications: (A) Zn sorbed to *Penicillium chrysogenum* at pH 6 (*15*); (B) zinc phytate solid (*21*); (C) zinc citrate dihydrate solid (*22*); (D) zinc acetate dihydrate solid (*15*); (E) zinc phosphate tetrahydrate solid, $Zn_3(PO_4)_2{\cdot}4H_2O$ (*21*); and (F) zinc phosphate dihydrate solid, $Zn_3(PO_4)_2{\cdot}2H_2O$ (*15*).

TABLE 1. Summary of Zn Sorption to Biofilm Data[a]

Sample	Zn sorption to biofilm (mol of Zn/kg of dry biosorbent) avg	2 std dev	EXAFS[b]
Zncell1	0.08	0.06	
Zncell2	0.13	0.09	
Zncell3	0.20	0.03	yes
Zncell4	0.31	0.01	yes
Zncell5	0.42	0.10	yes
Zncell6	0.50	0.07	yes
Zncell7	0.56	0.02	yes
Zncell8	0.64	0.12	yes
Zncell9	0.64	0.04	

[a] Dry biofilm weight (kilograms of dry biosorbent) was used to quantify the amount of solid biosorbent in sample suspensions and to normalize the sorption data. Sorption experiments were conducted with undried biofilm suspension. [b] Zinc K-edge EXAFS spectra were collected for samples Zncell3, Zncell4, Zncell5, Zncell6, Zncell7, and Zncell8.

Results and Discussion

Zn Sorption Experiment. The biofilm sorbed 0.08 ± 0.06 to 0.64 ± 0.04 mol of Zn (kg of biosorbent)$^{-1}$ from solutions having initial concentrations ranging from 4.8 to 301 μM Zn (Table 1). Equilibrium Zn concentrations in the range of 2.8−276 μM Zn were observed in this experiment. While these aqueous concentrations of Zn are too large to be representative of most pristine aqueous environments, they are well within the range of Zn concentrations encountered in contaminated aquatic environments, 0.05−1530 μM Zn (Table S-1 in the Supporting Information). The largest observed Zn loadings to the *P. putida* biofilm in this study were 0.64 ± 0.12 mol of Zn (kg of biosorbent)$^{-1}$ in sample Zncell8 and 0.64 ± 0.04 mol of Zn (kg of biosorbent)$^{-1}$ in sample Zncell9 (Table 1). The value of the largest observed Zn loading falls within the range of maximum values (0.1−2.0 mol kg^{-1}) reported for divalent metal sorption by other types of microbial biomass at pH 4.5−7.0 (*15*, *23*−*26*).

The adsorption isotherm data obtained from our experiments produced a characteristic L-curve when Zn loading to the biofilm (q, moles of Zn per kilogram of biosorbent) was plotted against the equilibrium Zn concentration (c, moles of Zn per kilogram of suspension) (Figure 1). A nonlinear least-squares fit to the adsorption data with the van Bemmelen−Freundlich equation (*13*), $q = Ac^{\beta}$, yielded $A = 30.09 \pm 8.18$ mol of Zn (kg of biosorbent)$^{-1}$ × [mol of Zn (kg of suspension)]$^{-\beta}$ and $\beta = 0.469 \pm 0.030$, respectively (±standard error), with the proportion of variance explained by the fit equal to 0.96. As there is no finite maximum value of q parametrized in the van Bemmelen−Freundlich equation, if Zn sorption by the biofilm has a maximum, it is greater than 1.01 mol of Zn (kg of biosorbent)$^{-1}$ (see Supporting Information). Although isotherm models do not provide mechanistic information about Zn speciation in our samples, they are useful for characterizing adsorption data.

Zn EXAFS Spectroscopy. The k^3-weighted Zn EXAFS spectra collected for samples with Zn loadings in the range of 0.20 ± 0.03 to 0.64 ± 0.12 mol of Zn (kg of biosorbent) are presented in Figure 2. These spectra are identical in phase

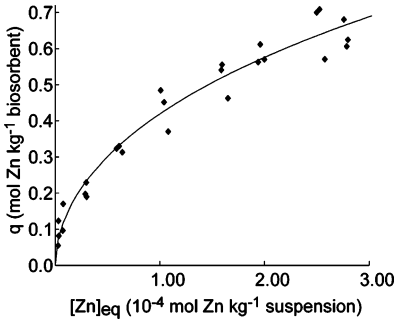

FIGURE 1. Zinc sorption to biofilm data (◆) is plotted with the nonlinear least-squares best fit (—) to the van Bemmelen−Freundlich model.

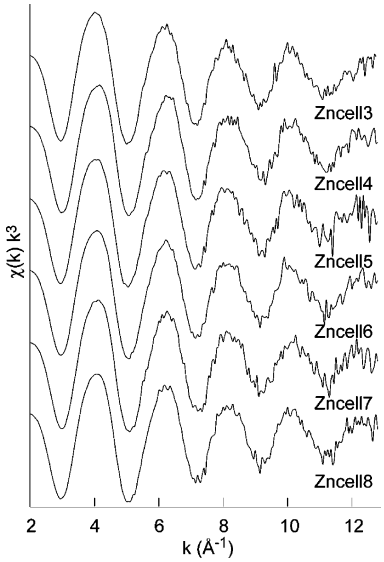

FIGURE 2. Summary of Zn K-edge EXAFS spectra collected for Zn sorbed to *P. putida* biofilm. Zinc loading to the biomaterial increases from sample Zncell3 to Zncell8; see Table 1 for loadings.

and amplitude (within spectral noise) and indicate that, over the range of Zn loadings studied, no significant changes in sorbed Zn speciation occurred. Zinc loading to the biofilm in the samples studied by EXAFS varied by a factor of 3. However, the samples represent Zn sorption by a biofilm in equilibrium with aqueous Zn concentrations that vary by a factor of 10.

First-shell fits to the experimental spectra provide clear evidence for Zn in tetrahedral coordination to O atoms: the number of nearest neighbors (N) was equal to 4.0 ± 0.12, and the distance between Zn and O atoms was equal to 1.97 ± 0.01 Å (Table 2). A representative experimental spectrum, Zncell7 [0.56 ± 0.02 mol of Zn (kg of biosorbent)$^{-1}$], is compared to those collected for reference materials zinc citrate, zinc acetate, Zn-sorbed *P. chrysogenum*, and zinc phytate in Figure 3a.

Citrate has three carboxyl groups per molecule, and in the solid zinc citrate dihydrate reference material presented here, $Zn_3(C_6H_5O_7)_2{\cdot}2H_2O$, there are two carboxyl groups per Zn atom. In the first shell of zinc citrate, Zn is octahedrally coordinated to O atoms with an interatomic distance of 2.04 Å (*22*). The difference between the local structure observed for zinc citrate and that of the tetrahedrally coordinated Zn in sample Zncell7 is clearly visible in the phase shift of the zinc citrate EXAFS spectrum to lower wavenumbers (k) relative to that of Zncell7 (Figure 3a). In zinc acetate, Zn is in octahedral coordination to first-shell O atoms, four O atoms from two acetate groups and two O atoms from water (*27*). The spectrum collected for zinc acetate (*15*) is shifted to lower k values relative to the spectrum from Zncell7 and exhibits a very different line-shape structure for all five oscillations displayed.

In the *P. chrysogenum* [0.24 mol of Zn (kg of dry biomaterial)$^{-1}$] reference material, Zn is tetrahedrally coordinated to O atoms and has two overlapping Zn−P pairs at 3.06 and 3.55 Å in the second shell (*15*) (Table 2). The Zn-sorbed *P. chrysogenum* spectrum provides a better approximation of the EXAFS spectrum of sample Zncell7 than do zinc citrate and zinc acetate (Figure 3a). There are, however, important differences between the spectra, particularly in the mismatches observed in the phase of the first oscillation and the line-shape symmetry of the second oscillation (Figure 3a). These differences are also evident in the second and third shells of the Fourier transforms, allowing

TABLE 2. First-Shell Fits to Representative Experimental Zn EXAFS Spectra Zncell3 and Zncell7[a] and Structural Details for Zn−P Reference Materials

		first O-shell			second P-shell		
sample name	Zn loading (mol of Zn/kg of biomass)	R_O (Å)	N_O	σ^2 (Å^2)	R_P (Å)	N_P	σ^2 (Å^2)
zinc phytate		1.98	4.0	0.006	3.12	0.9	0.008
					3.60	0.6	0.012
Zn *P. chrysogenum*[b]	0.24	1.99	2.3	0.00	3.06	0.7	0.00
					3.55	1.4	0.01
Zncell3	0.20	1.97	4.0	0.007			
Zncell7	0.57	1.96	4.0	0.007			

[a] The EXAFS fit values have errors equal to or less than ±0.01 Å for R_O, ±0.03 Å for R_P, 20% for N, and ±0.003 for σ^2 (Å^2). Zinc phytate EXAFS fit values are from ref *21*, Zn *P. chrysogenum* EXAFS fit values are from ref *15*, and Zncell3 and Zncell7 EXAFS fit values are from the present work. [b] In this fit $\Delta\sigma$ (Å) parameter was reported rather than σ^2 (Å^2).

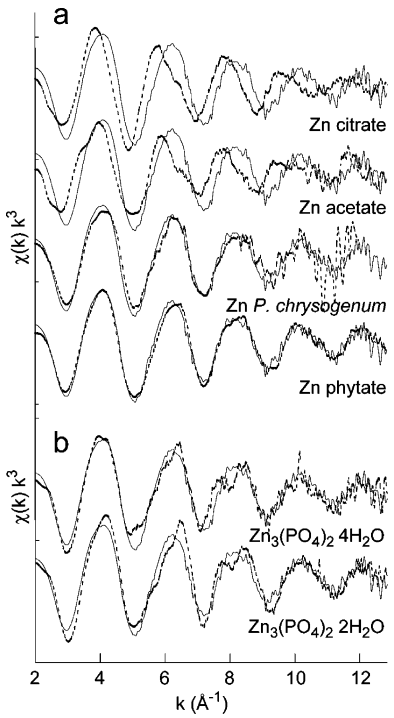

FIGURE 3. Experimental Zn EXAFS data collected for sample Zncell7 (solid lines) compared to reference spectra (---): (a) zinc citrate dihydrate (*22*), zinc acetate dihydrate (*15*), Zn sorbed *Penicillium chrysogenum* (*15*), and zinc phytate (*21*); (b) inorganic zinc phosphate compounds.

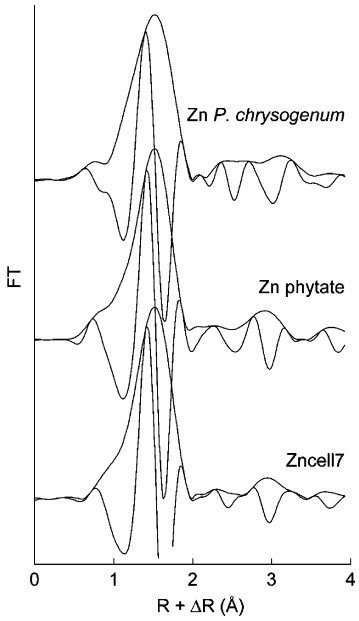

FIGURE 4. Fourier transform data for sample Zncell7 and reference materials zinc phytate and Zn sorbed to *P. chrysogenum*.

us to rule out the presence of two Zn−P shells at 3.06 and 3.55 Å in the *P. putida* sample (Figure 4).

Of the reference spectra surveyed, that of zinc phytate provided the best match to the Zncell7 spectrum (phytate is a cyclohexane hexaphosphate molecule). We observed improved spectral agreement in the phase of the first oscillation when compared to Zn *P. chrysogenum* (Figure 3a). Although the zinc phytate spectrum exhibits asymmetry in line shape of the second and third oscillations that is not present in the Zncell7 spectrum, the overall similarity between the zinc phytate and Zncell7 spectra suggests that Zn is predominantly complexed by organic phosphoryl groups in the unknown. In Figure 3b, the spectrum collected for sample Zncell7 is compared to those of two inorganic zinc phosphate compounds, $Zn_3(PO_4)_2{\cdot}4H_2O$ and $Zn_3(PO_4)_2{\cdot}2H_2O$. Neither reference spectrum provides a better match to the experimental spectrum than zinc phytate. Given the similarity between the Zncell7 and zinc phytate spectra, one and two Zn−P shell fits were performed for spectrum Zncell7. Although a two Zn−P shell fit was visually very good, it produced unreasonably large σ^2 values (ca. 0.03 Å^2). The fit results indicate that there may be other atomic pair shells in the region of 2.0−3.5 $R + \Delta R$ (angstroms), and perhaps greater structural disorder in the sample than in the zinc phytate reference.

Due to the apparent structural complexity of sample Zncell7, linear least-squares fits were performed with combinations of reference spectra, and the fit results are displayed in Table 3. A combination of zinc phytate and zinc citrate as component spectra representing Zn−phosphoryl and Zn−carboxyl species, respectively, produced the best fit (Figure 5). The best-fit results were 0.85 ± 0.10 zinc phytate and 0.23 ± 0.10 zinc citrate ($\chi_\nu^2 = 0.15$). The spectral contribution of zinc citrate to the two-component linear fit compensated for the asymmetry in the line shape of the second and third oscillations of the zinc phytate EXAFS spectrum relative to the biofilm spectrum (Figure 5a). Although the next best fit to the data was with 86 mol % zinc phytate and 23 mol % zinc acetate, the reduced χ_ν^2 parameter for the zinc acetate fit increased significantly (by 18%) over that of the zinc citrate fit (Table 3). The similarity in the results of the two-component zinc citrate and zinc acetate fits may result from the ratio of Zn atoms to carboxyl groups in the reference materials, 1:2 in both cases. On the basis of the linear least-squares fitting, we propose that the dominant Zn species present in Zn-sorbed *P. putida* samples at pH 6.9 and 0.20 mol of Zn (kg of dry biosorbent), and higher Zn loadings, is Zn−phosphoryl groups, with a lesser contribution to Zn sorption by carboxyl-type functional groups.

TABLE 3. Summary of Results for Two-Component Linear Least-Squares Fits to the Spectrum from Sample Zncell7

	zinc phytate	zinc acetate	zinc citrate	$Zn_3(PO_4)_2{\cdot}4H_2O$	$Zn_3(PO_4)_2{\cdot}2H_2O$
zinc phytate		0.86/0.23[a]	0.85/0.23	0.14/0.87	0.89/0.11
zinc acetate	**0.18**[b]		0.84/0.10	0.28/0.76	0.28/0.76
zinc citrate	**0.15**	**2.10**		0.27/0.75	0.22/0.78
$Zn_3(PO_4)_2{\cdot}4H_2O$	**0.20**	**0.33**	**0.36**		0.29/0.64
$Zn_3(PO_4)_2{\cdot}2H_2O$	**0.20**	**0.33**	**0.35**	**0.42**	

[a] The pairs of numbers presented in lightface type are the fitted proportions of the reference spectra for the two-component linear least-squares fit to the Zncell7 spectrum. The convention is *x*/*y*, where *x* is the fitted proportion of the reference spectrum on the left and *y* is the fitted proportion of the reference spectrum indicated in the column heading. [b] The numbers in boldface type are the χ_ν^2 values for two-component linear least-squares fits to the spectrum from sample Zncell7 with the two reference spectra indicated.

In support of our spectroscopic interpretation, many wet chemistry and modeling studies have proposed that phosphoryl and carboxyl groups are important in metal complexation by microbial cells (*15*, *23*, *26*, *28*−*30*). For example, Sarret et al. (*15*) examined Zn sorption to fungal cell walls at pH 6 as a function of Zn loading (0.0076−0.22 mol of Zn kg^{-1}). Zinc was predominantly associated with phosphoryl groups, and only at the highest Zn loading was a 5 mol % Zn association with carboxyl groups identified (*15*). Zinc sorption to *Bacillus subtilis* was best modeled as complexation to a combination of carboxyl and phosphoryl groups; Zn−carboxyl species were dominant at low pH, but the contribution of Zn−phosphoryl species increased as the pH approached circumneutral values (*23*). In another study, Zn sorption to bacterial cells was studied as a function of pH, and a two-site model (Zn−phosphoryl and Zn−carboxyl species) improved greatly the fit to their experimental sorption data over a one-site model (*28*).

Our EXAFS spectroscopic data do not allow us to identify the spatial location of Zn sorption within the biofilm. For example, we cannot distinguish Zn complexed to organic phosphate groups inside the cell or on the cell outer membrane from that outside the cell in the EPS. However, we can make some assumptions about where Zn is located on the basis of the known chemical composition of Gram-negative outer membranes and the typical components of lipopolysaccharides (LPS) and EPS. The outer membrane present in Gram-negative cells is composed of a phospholipid bilayer (Figure 6). The EPS for this culture, under these growth conditions has not been characterized but likely contains proteins, polysaccharides, uronic acids, nucleic acids, and lipids (*31*, *32*). Studies indicate that the polysaccharide components of EPS are a possible source of metal complexation by biofilms (*33*−*35*); however, our results suggest that the phosphoryl groups of the cell outer membrane are more important for Zn sorption at neutral pH than the carboxyl groups of the EPS or LPS. Although U sequestration by intracellular inorganic polyphosphates of *Acidithiobacillus ferrooxidans* biofilms has been observed (*36*), we rule out Zn sequestration by inorganic polyphosphates in this study because the Zn EXAFS spectra collected for our samples are very different from inorganic zinc phosphate reference materials and very similar to the organic zinc phytate and Zn *P. chrysogenum* reference materials (Figure 3b).

In the present study, carboxyl-type functional groups account for about 20 mol % of Zn species within the biofilm.

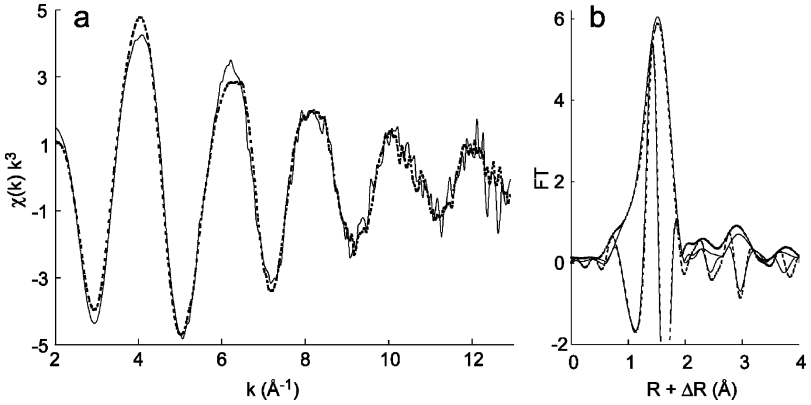

FIGURE 5. (a) Linear least-squares fit to experimental Zn EXAFS data collected for sample Zncell7, and (b) Fourier transform (magnitude and imaginary part) for experimental and fit data. The component spectra are zinc phytate and zinc citrate. (—) Experimental data; (---) fit to data.

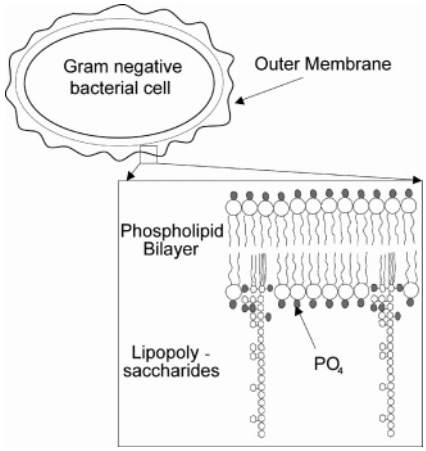

FIGURE 6. Outer membrane of Gram-negative cells is a possible source of Zn-complexing phosphoryl groups (adapted in part from ref *43*).

However, we cannot rule out a larger role for biofilm carboxyl groups in Zn complexation in other solution pH and growth conditions. The growth conditions used in this study (e.g., rich growth medium) may affect the amount and chemical character of the EPS present in our samples. While Gram-negative and Gram-positive bacterial cell surface chemistry appears to be independent of growth phase and nutrient-rich growth medium (*37*), bacterial EPS may be affected significantly by growth medium.

Given the spectroscopic evidence for Zn sorption by phosphoryl- and carboxyl-type functional groups, why does a two-term Langmuir model seem inappropriate for our data (see Supporting Information)? We hypothesize that this is a discrepancy in appearance only. First, it is important to remember that the Langmuir equation is an empirical model, and the affinity parameters calculated with the model do not necessarily correspond to specific sorbed species (*13*). Second, while XAS is an appropriate tool for characterizing the local atomic structure of Zn−biofilm complexes, it is only sensitive to the local structural environment of sorbed Zn. The consequence of using a local structure probe in a bioorganically complex biofilm is that the third-, fourth-, and fifth-shell atoms in the organic molecules, which may contribute to the metal-binding properties of the molecule, are difficult to resolve. The local structure sensitivity of XAS may act to simplify the number and type of categories to which Zn-complexing bioorganic functional groups can be attributed. For example, the phosphoryl binding sites of the biofilm likely have a number of specific molecular structures and affinities for Zn, but all are members of the Zn−phosphoryl complex group.

X-ray absorption spectroscopic studies of fungal cell walls (*15*), Gram-positive bacteria (*38*), and Gram-negative bacteria (present study) indicate that phosphoryl- and carboxyl-type functional groups are responsible for metal complexation by these three types of microorganisms despite the differences in molecular structure of their exterior surfaces. These results are consistent with studies that report very similar metal sorption properties for Gram-negative, Gram-positive, and mixtures of Gram-negative and -positive bacteria (*26*, *39*). They are also in agreement with the results of an infrared spectroscopic study of microbial surface functional groups that confirmed phosphoryl and carboxyl groups as those contributing to the negative surface charge of the bacteria studied in the pH range 4−9 (*37*). A universal character for the metal-complexing functional groups of microbial surfaces has been proposed and appears to be generally robust for many types and combinations of bacteria (*4*, *26*, *39*). The universality of the metal-complexation properties of bacteria seems to break down somewhat when bacterial consortia from contaminated environments are compared to those from natural−uncontaminated consortia and laboratory cultures (*6*). Borrok et al. (*6*) hypothesize that in situ selective pressures lead to bacterial consortia with Cd binding constants that vary by a factor of 10 and site densities that vary by a factor of 3. Given the emerging picture of a universal character of metal-complexing functional groups, we hypothesize that our spectroscopic Zn speciation results are generally representative of the types of metal-complexing functional groups present in natural biofilms. Spectroscopic examination of environmental samples is needed to confirm our hypothesis.

The literature detailing metal complexation by bacterial cells appears to present a fairly cohesive picture; however, the nature of metal complexation by bacterial EPS—either extracted or in the presence of cells—is more difficult to summarize. Although it is clear from the literature that bacterial EPS has significant metal-complexing capabilities, the wide variety of study approaches and experimental procedures (*33*−*36*), along with the variability in EPS production and characteristics for single cultures with different growth conditions (*40*, *41*) as well as among different cultures (*31*, *42*), makes comparisons among studies difficult. These difficulties are not unique to metal−biofilm studies but appear to apply to biofilm studies in general (*3*). As an example, eight different bacterial cultures isolated from the same activated sludge, and grown under the same conditions in the laboratory, exhibit different EPS compositions from one another and from the EPS extracted from the original activated sludge (*31*). The resulting number of Pb complex-

ation sites in that study ranged from 421 ± 44 to 2135 ± 55 μmol (g of EPS)$^{-1}$. In addition, the metal-complexing capability of bacterial EPS is affected by prior exposure of the bacteria to metals and the metal-resistant status of bacteria (*40*). For example, Cu-resistant bacteria isolated from Cu-contaminated soil produced EPS in response to Cu exposure (*9*). The studies discussed here point to the interdependence of EPS biochemical composition, genetics, and environmental conditions in controlling metal complexation by bacterial EPS. In the experiments presented here, the biofilm was formed in nutrient-rich, aerobic conditions in the absence of metal concentrations above those needed for growth. With respect to EPS metal-complexing character, we have examined one set of growth conditions among a very large set of possibilities. Future research of this type should strive to link spectroscopic evidence for metal-binding functional groups to specific environmental conditions that influence biofilm development and EPS characteristics.

Acknowledgments

B.T. and G.S. thank the National Science Foundation Collaborative Research Activities in Environmental Molecular Science (CRAEMS) program (Grant CHE-0089208), for funding. We thank Dr. Géraldine Sarret (CNRS) for providing Zn EXAFS reference spectra, Dr. Samuel Webb (Stanford Synchrotron Radiation Laboratory) for assistance with the use of SixPACK software, and Ms. Sirine Fakra (Advanced Light Source) for assistance with EXAFS data collection. The operation of the Advanced Light Source is supported by the Director, Office of Basic Energy Sciences of the U.S. Department of Energy under Contract DE-AC03-76SF00098.

Supporting Information Available

Data analysis methods, survey of Zn concentrations found in contaminated streams throughout the world, and a plot of the distribution coefficient K_d versus loading q. This material is available free of charge via the Internet at http://pubs.acs.org.

Literature Cited

(1) Costerton, J. W.; Lewandowski, Z.; Caldwell, D. E.; Korber, D. R.; Lappin-Scott, H. M. Microbial biofilms. *Annu. Rev. Microbiol.* **1995**, *49*, 711−745.

(2) Davey, M. E.; O'Toole, G. A. Microbial biofilms: from ecology to molecular genetics. *Microbiol. Mol. Biol. Rev.* **2000**, *64*, 847−867.

(3) Parsek, M. R.; Fuqua, C. Biofilms 2003: Emerging themes and challenges in studies of surface-associated microbial life. *J. Bacteriol.* **2004**, *186*, 4427−4440.

(4) Borrok, D.; Fein, J. B.; Kulpa, C. F. Proton and Cd adsorption onto natural bacterial consortia: testing universal adsorption behavior. *Geochim. Cosmochim. Acta* **2004**, *68*, 3231−3238.

(5) Daughney, C. J.; Siciliano, S. D.; Rencz, A. N.; Lean, D.; Fortin, D. Hg(II) adsorption by bacteria: A surface complexation model and its application to shallow acidic lakes and wetlands in Kejimkujik National Park, Nova Scotia, Canada. *Environ. Sci. Technol.* **2002**, *36*, 1546−1553.

(6) Borrok, D. M.; Fein, J. B.; Kulpa, C. F., Jr. Cd and proton adsorption onto bacterial consortia grown from industrial wastes and contaminated geologic settings. *Environ. Sci. Technol.* **2004**, *38*, 5656−5664.

(7) Fein, J. B.; Boily, J.-F.; Yee, N.; Gorman-Lewis, D.; Turner, B. F. Potentiometric titrations of *Bacillus subtilis* cells to low pH and a comparison of modeling approaches. *Geochim. Cosmochim. Acta* **2005**, *69*, 1123−1132.

(8) Farag, A. M.; Woodward, D. F.; Goldstein, J. N.; Brumbaugh, W.; Meyer, J. S. Concentrations of metals associated with mining waste in the sediments, biofilm, benthic macrovertebrates, and fish from the Coeur d'Alene River Basin, Idaho. *Arch. Environ. Contam. Toxicol.* **1998**, *34*, 119−127.

(9) Kunito, T.; Saeki, K.; Nagaoka, K.; Oyaizu, H.; Matsumoto, S. Characterization of copper-resistant bacterial community in rhizosphere of highly copper-contaminated soil. *Eur. J. Soil Biol.* **2001**, *37*, 95−102.

(10) Toner, B.; Manceau, A.; Webb, S. M.; Sposito, G. Zinc sorption to biogenic hexagonal-birnessite particles within a hydrated bacterial biofilm. *Geochim. Cosmochim. Acta* (accepted for publication).

(11) Villalobos, M.; Toner, B.; Bargar, J.; Sposito, G. Characterization of the manganese oxide produced by *Pseudomonas putida* strain MnB1. *Geochim. Cosmochim. Acta* **2003**, *67*, 2649−2662.

(12) Toner, B.; Fakra, S.; Villalobos, M.; Warwick, T.; Sposito, G. Spatially resolved characterization of biogenic manganese oxide production within the biofilm of *Pseudomonas putida* strain MnB1. *Appl. Environ. Microbiol.* **2005**, *71*, 1300−1310.

(13) Sposito, G. *The surface chemistry of natural particles*; Oxford University Press: New York, 2004.

(14) Marcus, M. A.; MacDowell, A.; Celestre, R.; Manceau, A.; Miller, T.; Padmore, H. A.; Sublett, R. E. Beamline 10.3.2 at ALS: a hard X-ray microprobe for environmental and material sciences. *J. Synchrotron Radiat.* **2004**, *11*, 239−247.

(15) Sarret, G.; Manceau, A.; Spadini, L.; Roux, J.-C.; Hazemann, J.-L.; Soldo, Y.; Eybert-Berard, L.; Menthonnex, J.-J. Structural determination of Zn and Pb binding sites in *Penicillium chrysogenum* cell walls by EXAFS spectroscopy. *Environ. Sci. Technol.* **1998**, *32*, 1648−1655.

(16) Webb, S. M. SIXPACK: A graphical user interface for XAS analysis using IFEFFIT. *Phys. Scr.* **2005**, *T115*, 1011−1014.

(17) Rehr, J. J.; Zabinsky, S. I.; Albers, R. C. High-order multiple-scattering calculations of X-ray absorption fine structure. *Phys. Rev. Lett.* **1992**, *69*, 3397−3400.

(18) Ravel, B. *EXAFS analysis using FEFF and FEFFIT*. A workshop with course materials available on CD-ROM at http://feff.Phys-.washington.edu/ravel/course/2000.

(19) Newville, M. IFEFFIT: interactive XAFS analysis and FEFF fitting. *J. Synchrotron Radiat.* **2001**, *8*, 332−324.

(20) Isaure, M. P.; Laboudigue, A.; Manceau, A.; Sarret, G.; Tiffreau, C.; Trocellier, P.; Lamble, G.; Hazemann, J. L.; Chateigner, D. Quantitative Zn speciation in a contaminated dredged sediment by μ-PIXE, μ-SXRF, EXAFS spectroscopy and principal component analysis. *Geochim. Cosmochim. Acta* **2002**, *66*, 1549−1567.

(21) Sarret, G.; Vangronsveld, J.; Manceau, A.; Musso, M.; D''Haen, J.; Menthonnex, J.-J.; Hazemann, J.-L. Accumulation forms of Zn and Pb in *Phaseolus vulgaris* in the presence and absence of EDTA. *Environ. Sci. Technol.* **2001**, *35*, 2854−2859.

(22) Sarret, G.; Saumitou-Laprade, P.; Bert, V.; Proux, O.; Hazemann, J.-L.; Traverse, A.; Marcus, M. A.; Manceau, A. Forms of zinc accumulated in the hyperaccumulator *Arabidopsis halleri*. *Plant Phys.* **2002**, *130*, 1815−1826.

(23) Fein, J. B.; Martin, A. M.; Wightman, P. G. Metal adsorption onto bacterial surfaces: Development of a predictive approach. *Geochim. Cosmochim. Acta* **2001**, *65*, 4267−4273.

(24) Wang, L.; Chua, H.; Zhou, Q.; Wong, P. K.; Sin, S. N.; Lo, W. L.; Yu, P. H. Role of cell surface components on Cu+2 adsorption by *Pseudomonas putida* 5-x from electroplating effluent. *Water Res.* **2003**, *37*, 561−568.

(25) Leung, W. C.; Wong, M.-F.; Chua, H.; Lo, W.; Yu, P. H. F.; Leung, C. K. Removal and recovery of heavy metals by bacteria isolated from activated sludge treating industrial effluents and municipal wastewater. *Water Sci. Technol.* **2000**, *41*, 233−240.

(26) Yee, N.; Fein, J. Cd adsorption onto bacterial surfaces: A universal adsorption edge? *Geochim. Cosmochim. Acta* **2001**, *65*, 2037−2042.

(27) Niekerk, J. N. v.; Schoening, F. R. L.; Talbot, J. H. The crystal structure of zinc acetate dihydrate, $Zn(CH_3COO)_2$ $2H_2O$. *Acta Crystallogr.* **1953**, *6*, 720.

(28) Ngwenya, B. T.; Sutherland, I. W.; Kennedy, L. Comparison of the acid−base behavior and metal adsorption characteristics of a gram-negative bacterium with other strains. *Appl. Geochem.* **2003**, *18*, 527−538.

(29) Seki, H.; Suzuki, A.; Mitsueda, S.-I. Biosorption of heavy metal ions on *Rhodobacter sphaeroides* and *Alcaligenes eutrophus* H16. *J. Colloid Interface Sci.* **1998**, *197*, 185−190.

(30) Kelly, S. D.; Kemner, K. M.; Fein, J. B.; Fowle, D. A.; Boyanov, M. I.; Bunker, B. A.; Yee, N. X-ray absorption fine structure determination of pH-dependent U-bacterial cell wall interactions. *Geochim. Cosmochim. Acta* **2002**, *66*, 3855−3871.

(31) Guibaud, G.; Comte, S.; Bordas, F.; Dupuy, S.; Baudu, M. Comparison of the complexation potential of extracellular polymeric substances (EPS), extracted from activated sludges and produced by pure bacteria strains, for cadmium, lead and nickel. *Chemosphere* **2005**, *59*, 629−638.

(32) Kachlany, S.; Levery, S.; Kim, J.; Reuhs, B.; Lion, L.; Ghiorse, W. Structure and carbohydrate analysis of the exopolysaccharide capsule of *Pseudomonas putida* G7. *Environ. Microbiol.* **2001**, *3*, 774−784.
(33) Jensen-Spaulding, A.; Cabral, K.; Shuler, M. L.; Lion, L. W. Predicting the rate and extent of cadmium and copper desorption from soils in the presence of bacterial extracellular polymer. *Water Res.* **2004**, *38*, 2231−2240.
(34) Sakairi, N.; Suzuki, S.; Ueno, K.; Han, S.-M.; Nishi, N.; Tokura, S. Biosynthesis of hetero-polysaccharides by *Acetobacter xylinum* − Synthesis and characterization of metal-ion adsorptive properties of partially carboxymethylated cellulose. *Carbohydr. Polym.* **1998**, *37*, 409−414.
(35) Salehizadeh, H.; Shojaosadati, S. A. Removal of metal ions from aqueous solution by polysaccharide produced from *Bacillus firmus*. *Water Res.* **2003**, *37*, 4231−4235.
(36) Merroun, M.; Hennig, C.; Rossberg, A.; Gelpel, G.; Reich, T.; Selenska-Pobell, S. Molecular and atomic analysis of uranium complexes formed by three eco-types of *Acidithiobacillus ferrooxidans*. *Biochem. Soc. Trans.* **2002**, *30*, 669−671.
(37) Wei, J.; Saxena, A.; Song, B.; Ward, B. B.; Beveridge, T. J.; Myneni, S. C. B. Elucidation of functional groups on Gram-positive and Gram-negative bacterial surfaces using infrared spectroscopy. *Langmuir* **2005**, *20*, 11433−11442.
(38) Boyanov, M. I.; Kelly, S. D.; Kemner, K. M.; Bunker, B. A.; Fein, J. B.; Fowle, D. A. Adsorption of cadmium to *Bacillus subtilis* bacterial cell walls: A pH-dependent X-ray absorption fine structure spectroscopy study. *Geochim. Cosmochim. Acta* **2003**, *67*, 3299−3311.
(39) Yee, N.; Fein, J. B. Quantifying metal adsorption onto bacteria mixtures: A test and application of the surface complexation model. *Geomicrobiol. J.* **2003**, *20*, 43−60.
(40) Kazyl, S. K.; Sar, P.; Singh, S. P.; Sen, A. K.; D'Souza, S. F. Extracellular polysaccharides of a copper-sensitive and a copper-resistant *Pseudomonas aeruginosa* strain: Synthesis, chemical nature and copper binding. *World J. Microbiol. Biotechnol.* **2002**, *18*, 583−588.
(41) Thormann, K. M.; Saville, R. M.; Shukla, S.; Pelletier, D. A.; Spormann, A. M. Initial phases of biofilm formation in *Shewanella oneidensis* MR-1. *J. Bacteriol.* **2004**, *186*, 8096−8104.
(42) Templeton, A. S.; Spormann, A. M.; Brown, G. E., Jr Speciation of Pb(II) sorbed by *Burkholderia cepacia*/goethite composites. *Environ. Sci. Technol.* **2003**, *37*, 2166−2172.
(43) Madigan, M.; Martinko, J.; Parker, J. *Brock Biology of Microorganisms*, 9th ed.; Prentice-Hall: Upper Saddle River, NJ, 2000.

Received for review March 17, 2005. Revised manuscript received July 28, 2005. Accepted August 22, 2005.

ES050528+